NAVAL POSTGRADUATE SCHOOL

MONTEREY, CALIFORNIA

THESIS

ANALYSIS OF AC LOW-VOLTAGE ENERGY HARVESTING

by

Dmitry Shvets

September 2014

Thesis Advisor: Alexander L. Julian
Second Reader: Giovanna Oriti

Approved for public release; distribution is unlimited

THIS PAGE INTENTIONALLY LEFT BLANK

REPORT DOCUMENTATION PAGE

Form Approved OMB No. 0704-0188

1. AGENCY USE ONLY ***(Leave blank)***	**2. REPORT DATE** September 2014	**3. REPORT TYPE AND DATES COVERED** Master's Thesis

4. TITLE AND SUBTITLE
ANALYSIS OF AC LOW-VOLTAGE ENERGY HARVESTING

5. FUNDING NUMBERS

6. AUTHOR(S) Dmitry Shvets

7. PERFORMING ORGANIZATION NAME(S) AND ADDRESS(ES)
Naval Postgraduate School
Monterey, CA 93943-5000

8. PERFORMING ORGANIZATION REPORT NUMBER

9. SPONSORING /MONITORING AGENCY NAME(S) AND ADDRESS(ES)
N/A

10. SPONSORING/MONITORING AGENCY REPORT NUMBER

11. SUPPLEMENTARY NOTES The views expressed in this thesis are those of the author and do not reflect the official policy or position of the Department of Defense or the U.S. Government. IRB Protocol number ____N/A____.

12a. DISTRIBUTION / AVAILABILITY STATEMENT
Approved for public release; distribution is unlimited

12b. DISTRIBUTION CODE
A

13. ABSTRACT (maximum 200 words)

Piezoelectricity is a material property that generates an electric charge proportional to the mechanical stress placed on the material. This phenomenon was first discovered by the Curie brothers in 1880. This material property gives the ability to turn vibrations into an electrical waveform, but power electronics is necessary to harness this low-level energy.

AC power is often produced at the power plant level in modern society; however, low voltage AC power is widely available in vibrational form. The U.S. Navy may be able to utilize piezoelectric technology to harness wasted vibrational energy. Some of these applications include inserting a piezoelectric harvester in shoes to supply small amounts of power to cell phones or utilizing motion energy to provide power to iPod chargers.

The power electronics that provides full bridge rectification and step down conversion, which achieves AC-DC power harvesting, is discussed. Also discussed is a breakdown of possible applications for such a device as well as the benefits of turning AC power into DC. A Linear Technology LTC-3588-1 integrated circuit was simulated in software and demonstrated in hardware. The hardware experiment showed that the software accurately predicted the performance of the chip.

14. SUBJECT TERMS Renewable energy, Piezoelectric, Energy harvesting, buck converter

15. NUMBER OF PAGES
59

16. PRICE CODE

17. SECURITY CLASSIFICATION OF REPORT	**18. SECURITY CLASSIFICATION OF THIS PAGE**	**19. SECURITY CLASSIFICATION OF ABSTRACT**	**20. LIMITATION OF ABSTRACT**
Unclassified	Unclassified	Unclassified	UU

NSN 7540-01-280-5500

Standard Form 298 (Rev. 2-89)
Prescribed by ANSI Std. 239-18

THIS PAGE INTENTIONALLY LEFT BLANK

Approved for public release; distribution is unlimited

ANALYSIS OF AC LOW-VOLTAGE ENERGY HARVESTING

Dmitry Shvets
Lieutenant, United States Navy
B.S., United States Naval Academy, 2008

Submitted in partial fulfillment of the
requirements for the degree of

MASTER OF SCIENCE IN ELECTRICAL ENGINEERING

from the

NAVAL POSTGRADUATE SCHOOL
September 2014

Author: Dmitry Shvets

Approved by: Alexander L. Julian
Thesis Advisor

Giovanna Oriti
Second Reader

R. Clark Robertson
Chair, Department of Electrical and Computer Engineering

THIS PAGE INTENTIONALLY LEFT BLANK

ABSTRACT

Piezoelectricity is a material property that generates an electric charge proportional to the mechanical stress placed on the material. This phenomenon was first discovered by the Curie brothers in 1880. This material property gives the ability to turn vibrations into an electrical waveform, but power electronics is necessary to harness this low-level energy.

AC power is often produced at the power plant level in modern society; however, low voltage AC power is widely available in vibrational form. The U.S. Navy may be able to utilize piezoelectric technology to harness wasted vibrational energy. Some of these applications include inserting a piezoelectric harvester in shoes to supply small amounts of power to cell phones or utilizing motion energy to provide power to iPod chargers.

The power electronics that provides full bridge rectification and step down conversion, which achieves AC-DC power harvesting, is discussed. Also discussed is a breakdown of possible applications for such a device as well as the benefits of turning AC power into DC. A Linear Technology LTC-3588-1 integrated circuit was simulated in software and demonstrated in hardware. The hardware experiment showed that the software accurately predicted the performance of the chip.

THIS PAGE INTENTIONALLY LEFT BLANK

TABLE OF CONTENTS

THIS PAGE INTENTIONALLY LEFT BLANK

LIST OF FIGURES

LIST OF TABLES

THIS PAGE INTENTIONALLY LEFT BLANK

LIST OF ACRONYMS AND ABBREVIATIONS

AC	Alternating Current
C	Capacitor
CCM	Continuous Conduction Mode
D	Duty Cycle
DC	Direct Current
DCM	Discontinuous Conduction Mode
F_s	Frequency
GND	Ground
Hz	Hertz
I	Current
I_{bridge}	Diode Bridge Current
L	Inductor
LTSPICE	Linear Technology Simulation Program with Integrated Circuit Emphasis
NMOS	n-type metal-oxide-semiconductor field-effect transistor
P	Power
PMOS	p-type metal-oxide-semiconductor field-effect transistor
R	Resistor
R_{load}	Load Resistance
S	Switch
UVLO	Under-Voltage Lockout
V_{peak}	Peak Voltage
V_{pp}	Peak-to-Peak Voltage
$V_{pzinput}$	Piezoelectric Input Voltage
V_s	Voltage Source

THIS PAGE INTENTIONALLY LEFT BLANK

EXECUTIVE SUMMARY

AC energy harvesting has not been the focal point of industry in the last few years. This untapped sector has the potential to save the consumer money as well as save the power generation companies the need to build more power plants. The Department of Defense (DOD) has the opportunity to improve the reliability of components, create energy savings and develop an alternative option for backup power or secondary power.

In the DOD as well as the private sector, with an ever growing energy demand, taking steps to capture wasted energy is essential for our energy security. We have seen such efforts in car manufacturing, such as the Prius, that returns energy to the battery through the use of its regenerative brake system. Power electronics is the critical technology that makes harvesting this unused energy possible.

Piezoelectricity is a material property that generates an electric charge proportional to mechanical stress. This phenomenon was first discovered by the Curie brothers in 1880. This material property can be used to turn vibrational force into an electrical signal. While the low power level signals are useless by themselves, incorporating power electronics to transform this waveform into energy stored on a battery is useful.

The technologies discussed in this research are the full-bridge rectifier, buck chopper, and hysteresis control of power conversion. Utilizing these techniques, we can transform an AC waveform into energy stored in a battery. The simulated source used for the research was a typical AC sine wave from a floating function generator. A simulated input allowed the designer the tools needed to identify the piezoelectric device behavior desired for a specific application.

Applications of this device include storing vibrational energy in a battery and sensing a change in vibrational energy of a monitored device. In the case of motors, vibrations are an unwanted byproduct, and if abnormal vibrations are detected, it may indicate that maintenance should be performed prior to equipment failure.

A Linear Technologies Demonstration Board, 1459B, was used with a LTC3588EMSE-1 integrated circuit. The demonstration board was simulated in software to predict the performance and then tested in hardware. This link between software design and hardware verification is a stepping stone towards a cost efficient design. The more accurate the software design model is, the less money is wasted on building prototypes that do not work as desired when fabricated.

ACKNOWLEDGMENTS

I would like to thank Professor Julian for supporting me in this project, and Professor Oriti for taking time out of her day to assist me. I would like to thank the U.S. Navy for giving me the opportunity to do research in a field that both interests me and has benefits for the Navy. And most of all, I would like to thank my wife and daughters who have supported me throughout my career.

THIS PAGE INTENTIONALLY LEFT BLANK

I. INTRODUCTION

Vibrations are part of everyday life, from the vibrations of the engine when you drive to work to the ceiling fan that works twenty-four hours a day circulating the air in your house. Until the discovery of the piezoelectric phenomenon, this form of energy remained useless. This research into the performance of a piezoelectric harvester is intended to showcase the capabilities as well as verify the specification sheet describing a particular integrated circuit. Linear Technologies provided a simulation model of their product, and this model's performance is compared against hardware performance.

A. AUTHORITY AND IMPORTANCE TO CONDUCT ENERGY RESEARCH

The Secretary of the Navy's concern for our energy security has prompted the release of SECNAV INSTRUCTION 4101.3 [1] and the establishment of the Task Force Energy Charter [2]. In the charter, the Deputy Chief of Naval Operations for Fleet Readiness and Logistics (CNO N4) is charged with developing a Navy Energy Strategy. This is done by the establishment of the seven working groups that focus on key mission areas. Research in energy is done on a partnership basis due to the vastness of the information age. According to the Secretary of the Navy, the Honorable Ray Mabus,

> The Navy's partnership with the Naval Postgraduate School helps prepare our future leaders to integrate energy efficiencies and alternative energy into strategy and operations, which will strengthen our energy security. [3]

This emphasis on the importance for energy research motivated this research.

B. OBJECTIVE

The Linear Technologies LTC3588EMSE-1 integrated circuit is the focal point of this research. This commercially available energy harvester is tested through a demonstration board integration structure (Demonstration Circuit 1459B). A piezoelectric source is simulated with a floating function generator to provide test case scenarios for various frequency and voltage inputs. Linear Technologies created the LTSpiceIV program to showcase their product in a simulation environment. A work bench test was

set up to compare the simulation results against hardware measurements to demonstrate the reliability of software design.

C. PREVIOUS WORK

Harvesting power from a solar cell source was considered in [4]. The research focused on testing the BQ25504 Texas Instruments chip that harvested power on a milliwatt (mW) scale. Miniature electromechanical generation via motion to create power was examined in [5]. Motion energy is something we see and use on a daily basis but not for storing energy for later electrical use, except in the case of wristwatches that already utilize piezoelectric technology. A third Naval Postgraduate School student experimented with vibrational energy, highlighting the advantage of piezoelectric properties for collecting vibrational energy [6]. The next logical step is to simulate an AC voltage source to use as input to the energy harvester, since the piezoelectric element can be tailored to the application. Power converters have been used to charge a battery using a piezoelectric energy source [7]. These converters are slightly different than the integrated circuit studied in this thesis. In [8], a piezoelectric source was used to charge a wireless remote power supply. In this thesis, a function generator is used to test the behavior of the integrated circuit. The purpose of this research is to bridge the previous thesis concepts together into an analysis of the Linear Technology LTC-3588-1 chip used to harvest piezoelectric energy from vibrations.

D. THESIS ORGANIZATION

The previous work and motivation for this research was covered in this chapter. The two key power electronic functions, full bridge rectification and buck converter operation, which makes this design viable, are covered in Chapter II. The simulation is covered in Chapter III, with the simulation results and hardware measurements discussed in Chapter IV. The conclusion, as well as future work recommendations, are in Chapter V.

II. POWER ELECTRONICS THAT MAKES AC ENERGY HARVESTING POSSIBLE

The piezoelectric energy conversion process produces DC power from an AC source, requiring the AC input to first be converted to a DC signal. The current draw by the DC load from the integrated circuit follows Ohm's law $V = IR$, since the load considered in this thesis is a resistive. The input to the LTC-3588-1 integrated circuit is a variable AC sine wave simulating a piezoelectric source. Voltage regulation is accomplished with a buck chopper. The buck chopper turns the current on and off with respect to the changing voltage in order to regulate the output voltage.

A typical diode rectifier is shown in Figure 1a. The characteristics of voltage source v_s, the current i, and the diode voltage v_d are shown in Figure 1b. This application is not very useful due to the large ripple; however, we see that both v_d and i have an average DC component.

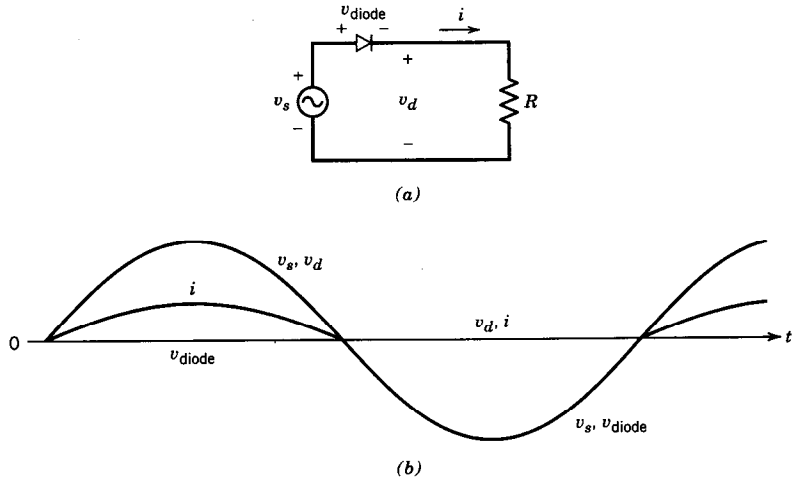

Figure 1. Simple diode rectifier circuit and waveforms (from [9]).

A more practical application is the full bridge diode rectifier shown in Figure 2 with the equivalent circuit shown in Figure 3. In the equivalent circuit, we analyze the

state variables, the inductor current i_s and the capacitor voltage v_d. Referring to Figure 3, using Kirchhoff's voltage law (KVL), when i_d is not zero, we obtain

$$| \mathrm{v}_s | = R_s i_d + L_s \frac{di_d}{dt} + v_d, \tag{1}$$

and with Kirchhoff's current law (KCL), we obtain

$$i_d = C_d \frac{dv_d}{dt} + \frac{v_d}{R_{load}}. \tag{2}$$

Using PSpice simulation software to simulate the circuit in Figure 2, we obtain the output waveforms shown in Figure 4.

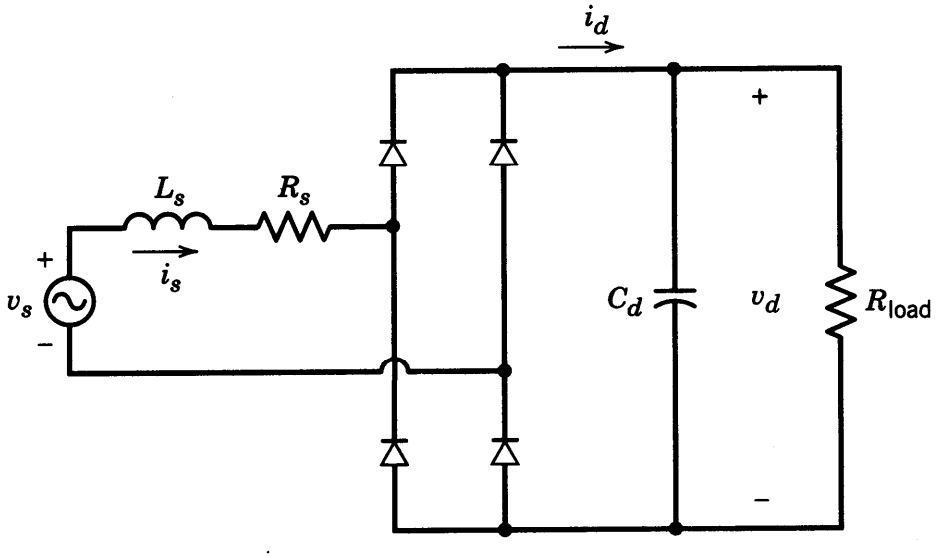

Figure 2. Practical full bridge rectifier (from [9]).

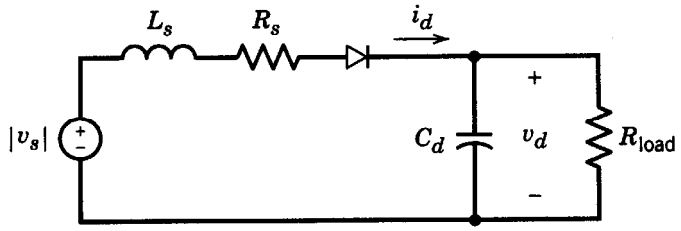

Figure 3. Equivalent circuit for Figure 2 (from [9]).

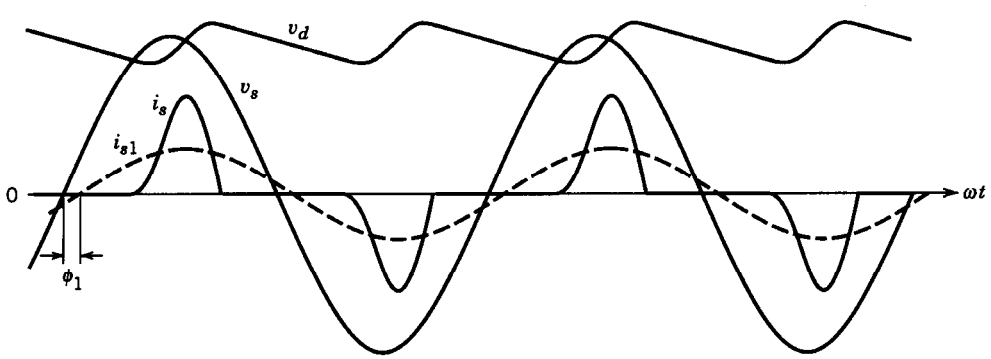

Figure 4. PSpice waveform from full bridge rectifier in Figure 2 (from [9]).

The end result of this full bridge rectifier is a DC voltage v_d as shown in Figure 4. Now that the voltage is DC, the next process is to step the voltage down to regulate the output voltage.

A. BUCK CHOPPER

One way to step down a voltage is to use a voltage divider, as shown in Figure 5. This approach has the cost of losses due to the resistors dissipating power. This approach also does not regulate the output voltage due to the resistor having a fixed value. The voltage divider output in Figure 5 is given by

$$V_{out} = \frac{V_{in} R_2}{R_1 + R_2}. \tag{3}$$

This topology steps down voltage but, due to its inability to regulate the voltage, it only fixes one of the problems while causing excess power losses. The efficient, more modern, way to step down a voltage is by utilizing the circuit topology known as the buck chopper, also called a step-down converter. A buck chopper also regulates the output voltage.

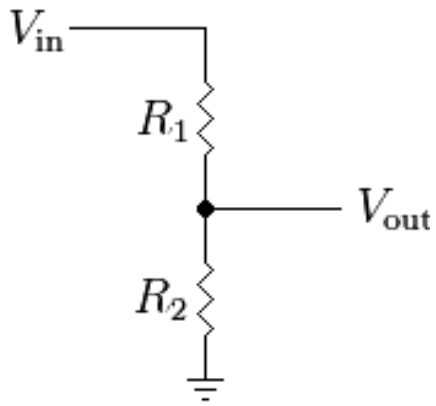

Figure 5. Typical voltage divider.

A typical buck chopper is shown in Figure 6 [10]. Three basic elements make up the buck chopper: a switching element, a diode and an inductor. The input is a voltage source *E*. The output current i_L divides between the load resistance *R* current i_R and the filter capacitor *C* current i_C. The capacitive filter is in parallel with the load resistor *R*. This circuit maintains a fixed voltage utilizing feedback control of the duty cycle *D* of the solid state switch S. We pick a value of *C* large enough so that V_C has negligible AC ripple.

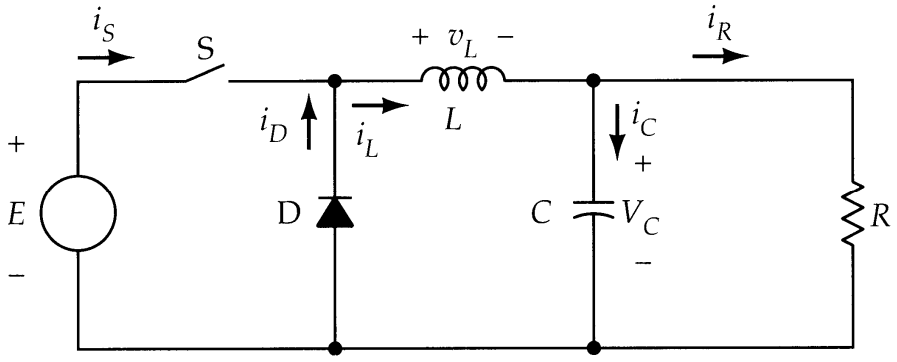

Figure 6. Conventional buck chopper (from [10]).

The two conduction modes of the buck chopper are continuous conduction mode (CCM) and discontinuous conduction mode (DCM). In order to be in CCM, the inductor current must never drop to zero, putting constraints on the ripple current. The values of the inductance L and resistance R must satisfy [10]

$$L \geq \frac{R}{2f}(1-D), \tag{4}$$

where D is the duty cycle and f is the switching frequency. The duty cycle D is the proportion of a switching period $1/f$ that the switch is closed.

The two cases of the buck chopper are with the switch either open or closed, as shown in Figure 7. When the switch is closed, $E = v_L + V_C,$ and

$$E = L\frac{di_L}{dt} + V_C \rightarrow \frac{di_L}{dt} = \frac{E - V_C}{L} \rightarrow di_L = \frac{E - V_C}{L}dt. \tag{5}$$

Integrating both sides of (5) over one switching period yields

$$I_{\max} - I_{\min} = \frac{E - V_C}{L}DT \tag{6}$$

where $I_{\max}$ is the maximum inductor current and $I_{\min}$ is the minimum inductor current.

When the switch is open and the diode is conducting, $v_L + V_C = 0,$ and

$$0 = L\frac{di_L}{dt} + V_C \rightarrow \frac{di_L}{dt} = -\frac{V_C}{L} \rightarrow di_L = -\frac{V_C}{L}dt. \tag{7}$$

Integrating both sides of (7) over one switching period yields

$$I_{\min} - I_{\max} = -\frac{V_C}{L}(1-D)T. \tag{8}$$

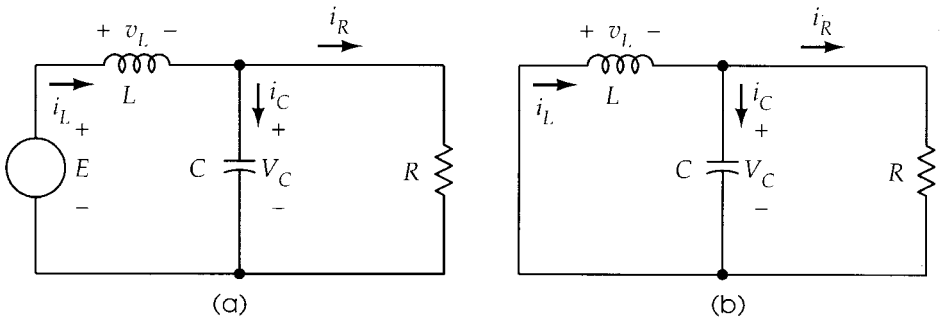

Figure 7. Buck chopper switch open (a), switch closed (b) (from [10]).

The relationship between the output voltage and input voltage is calculated by equating (6) and (8):

$$\frac{E-V_C}{L}DT=\frac{V_C}{L}(1-D)T \tag{9}$$

which simplifies to

$$V_C = DE. \tag{10}$$

The output voltage regulation V_C is based upon the duty cycle and the input voltage *E*. The average inductor current is the average of $I_{\max}$ and $I_{\min}$ and equals the average load current

$$avg(i_L)=avg(i_R) \tag{11}$$

where

$$avg(i_R)=\frac{avg(V_C)}{R}. \tag{12}$$

Figure 8 shows the relationship between duty cycle and current in continuous conduction mode.

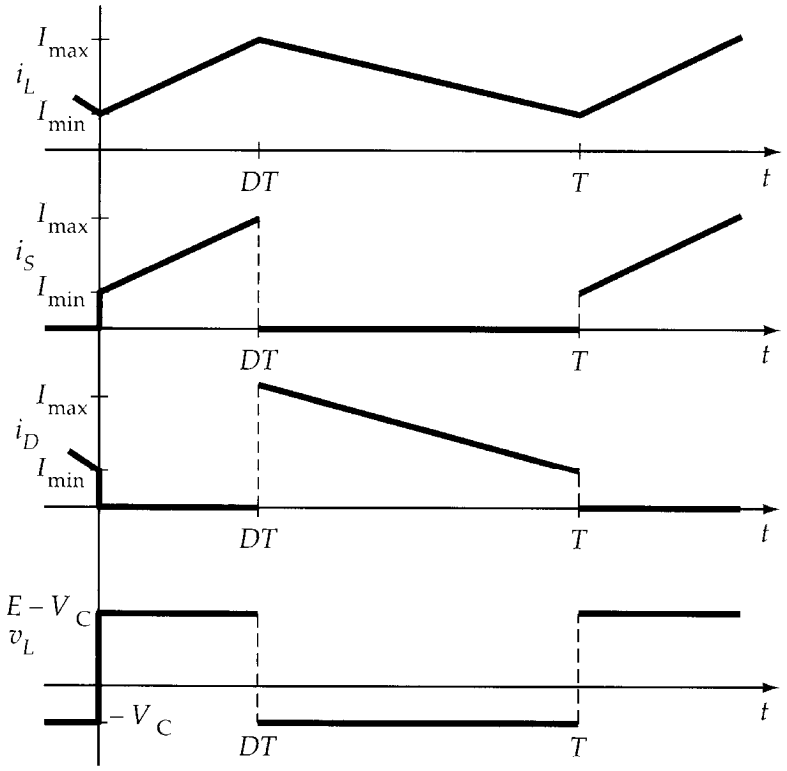

Figure 8. The relationship between the duty cycle and current (from [10]).

In the DCM $I_{min} = 0$, and I_{max} is defined by (6). The peak current I_{max} is [10]

$$I_{max} = \frac{V_C}{L}(D_2 - D)T \tag{13}$$

where D_2 is the duty cycle of the discontinuous mode as shown in Figure 9. In the case of DCM, the DC inductor current is not large enough to stay in continuous conduction, and this causes the current to fall to zero for a period of time each switching period. This puts the converter into the DCM. The inductor current in the DCM is shown in Figure 9.

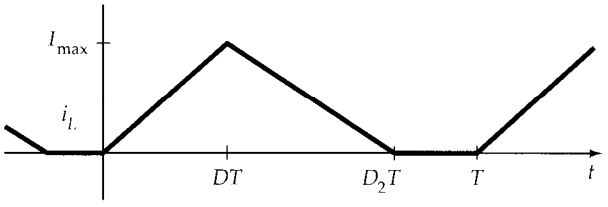

Figure 9. DCM current behavior of the inductor current (from [10]).

A graph of the voltage ratio versus the duty cycle for both the CCM and DCM is shown in Figure 10. The discontinuous region is nonlinear with respect to the duty cycle.

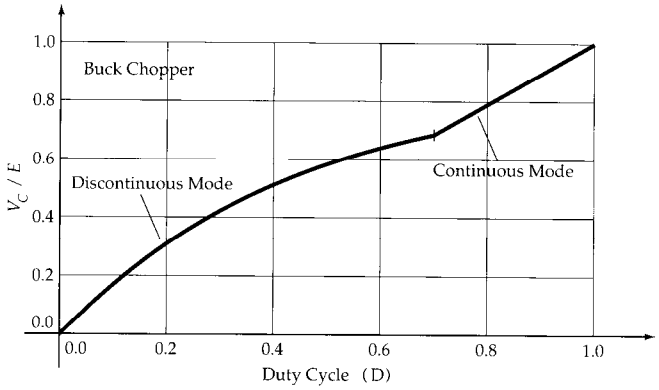

Figure 10. Buck chopper modes with respect to duty cycle (from [10]).

This pulsed approach allows a buck chopper to regulate the output voltage more efficiently than the resistor divider architecture. With no resistors in the power conversion topology between the input voltage source and the load, the circuit is more efficient than a resistor divider.

With the output voltage regulated, power can be harvested at the load. Integrating the rectifier concept and the buck chopper concept together converts an AC signal to a DC signal regulated to a predetermined voltage value. This is done with the LTC-3588-1 piezoelectric energy harvester [11]. The LTC-3588-1 is mounted on an integrated circuit demonstration board 1459B [12]. This board was chosen due to the ability to swap out components as well as the availability of Linear Technology's simulation model for this board.

III. SIMULATION ANALYSIS OF PIEZOELECTRIC ENERGY HARVESTER

The PSpice simulation of the demonstration board containing the energy harvesting integrated circuit is described in this chapter. Linear Technologies has created its own version of PSpice, called LTSpiceIV. This program is available from Linear Technologies' website, along with a model demonstration board circuit 1459B, and a graphical user interface, as shown in Figure 11.

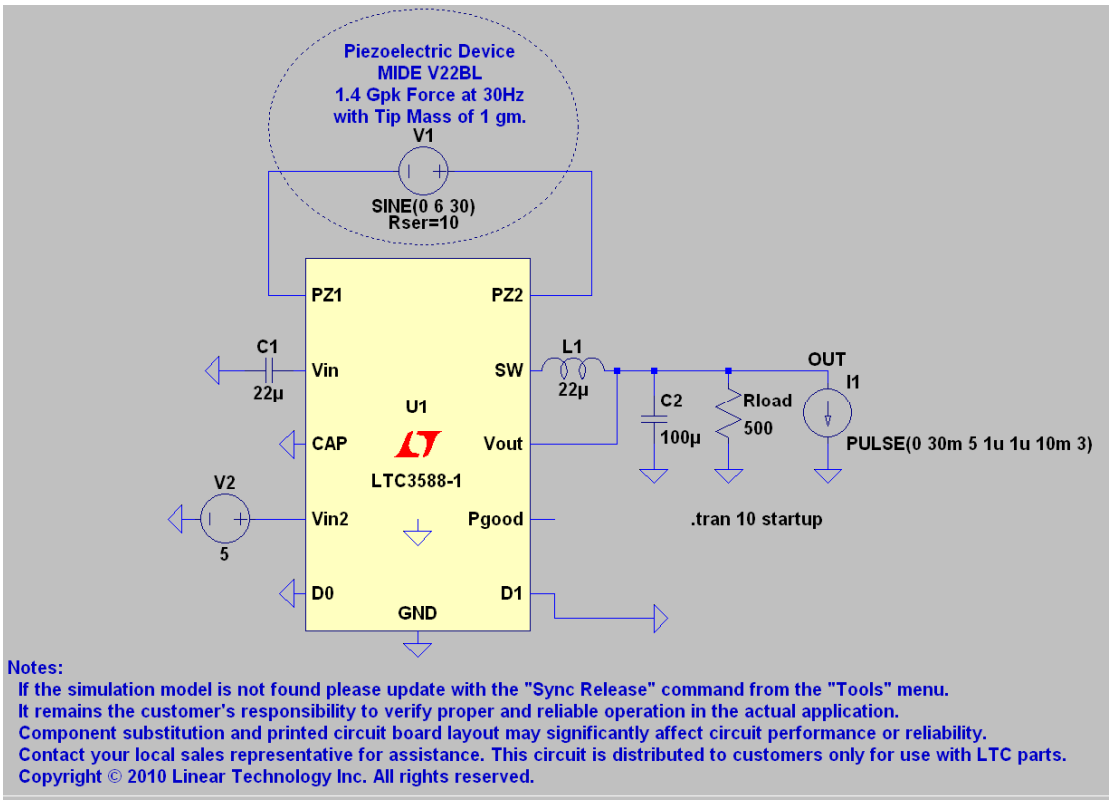

Figure 11. LTSpiceIV model of demonstration board (from [12]).

The setup of the simulation includes a 500 Ω R_{load} and a 6.0 V peak AC source at 30 Hz connected to pins PZ1 and PZ2 of the integrated circuit simulation. The outputs of the simulation include the output voltage, the output voltage ripple, the switching waveforms and the output current. All parameters of this model can be modified except the LTC3588-1 chip. Both D0 and D1 pins are grounded to choose the 1.8 V regulation

operating mode. The inductor L_1 and capacitors C_1 and C_2 are set to match the demonstration board used in bench testing. The load current pulse is off for the simulations shown in this thesis and is not present on the demonstration board. The capacitor C_1, shown in Figure 11, is the DC bus capacitor after diode rectification of the AC input. The voltage source V_2 is the 5.0 V supply for the integrated circuit.

A. SIMULATED OUTPUT VOLTAGE

The simulated output voltage has a calculated ripple of 47.0 mV, as shown in Figure 12. The average simulated DC voltage is 1.81 V. The input, as shown in Figure 11, is a sine wave at 30 Hz. The D0 and D1 jumpers are connected to ground, which puts the device in the 1.8 V output voltage setting.

Figure 12. The simulated output voltage with a 500 Ω load is measured at the V_{out} test point, as shown in Figure 11.

Modifying the jumpers D0 and D1 by connecting them to 0.0 V or 5.0 V produces four different output voltages, 1.8 V, 2.5 V, 3.3 V and 3.6 V, in the simulation. These different voltages are chosen based on the battery or device being charged with this energy harvester.

B. SIMULATED OUTPUT CURRENT

The simulated output current into the 500 Ω load of the circuit shown in Figure 11 is shown in Figure 13. The average DC current was measured to be 3.6 mA. The simulation shows a slight AC ripple in the output. Using $P = IV$, we calculate a simulated power generation of 6.48 mW.

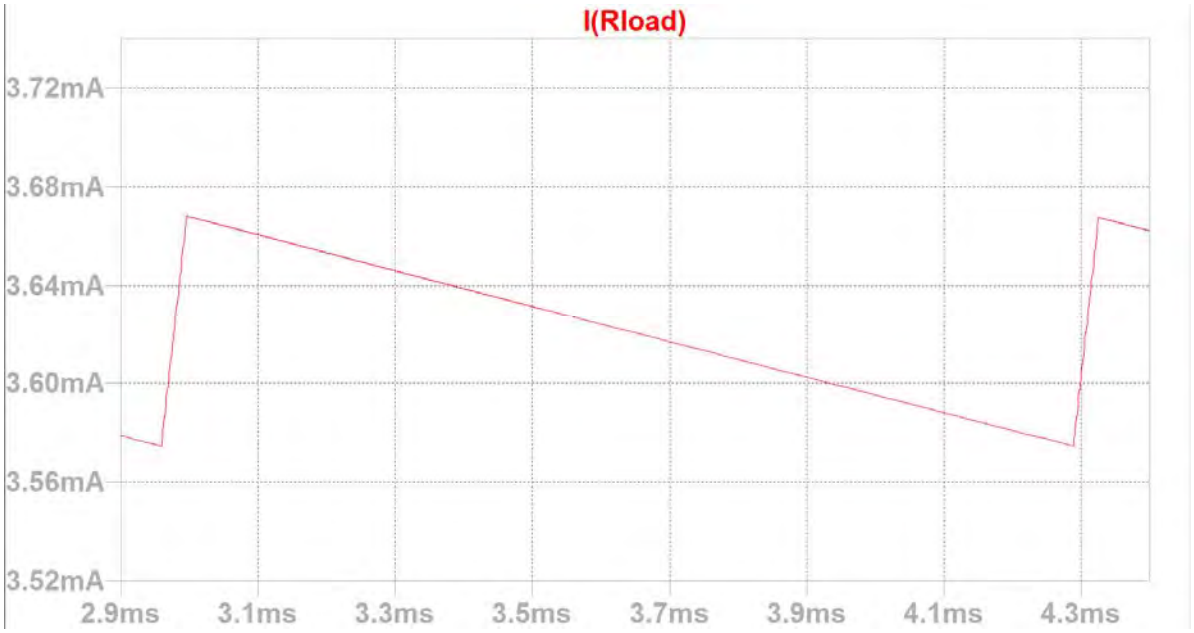

Figure 13. Simulated output current measured into the load resister shown in Figure 11.

C. BUCK CONVERTER SWITCHING WAVEFORM

The datasheet included oscilloscope waveforms showing the typical operation of the chip. The measured switching waveform from the datasheet is shown in Figure 14 and matches the simulated waveforms shown in Figure 15 and Figure 16. We expect to get the same correlation between the simulation and our laboratory measurements.

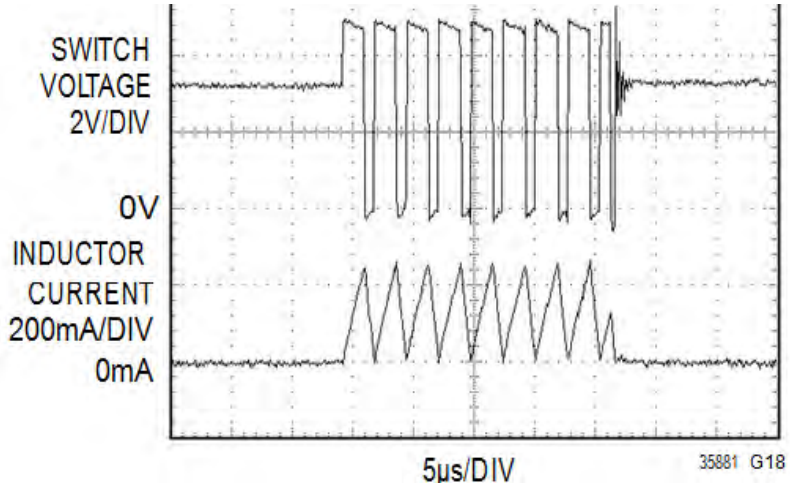

Figure 14. Switching waveform shown in the datasheet (from [11]).

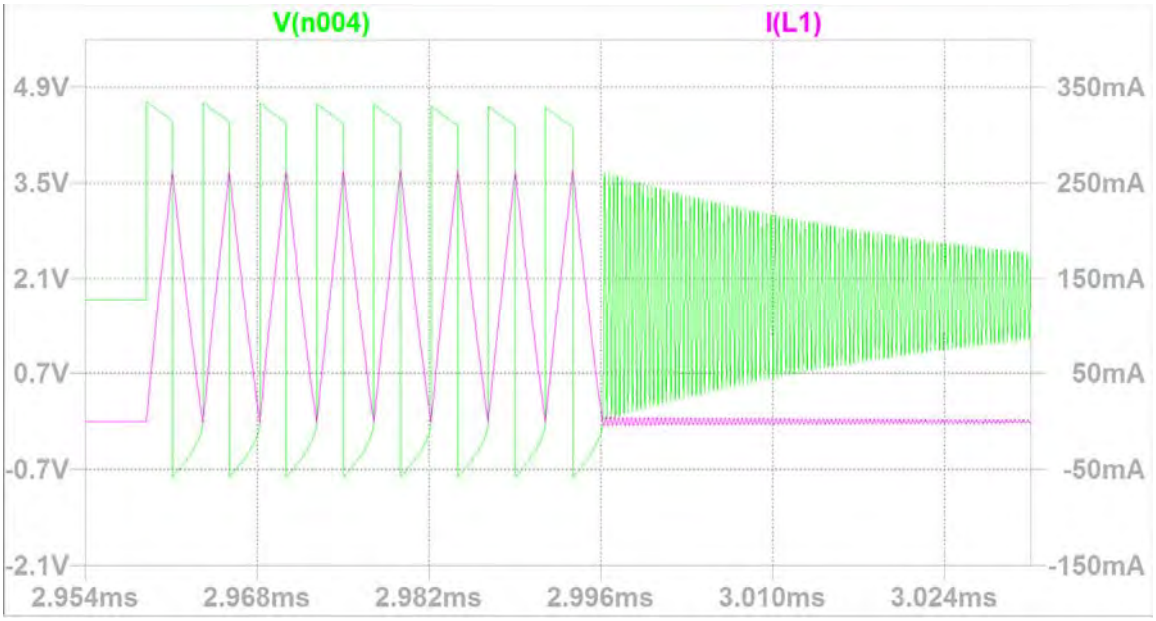

Figure 15. Simulated switching waveforms from LTSpiceIV (measured voltage from SW pin and current through L_1 shown in Figure 11).

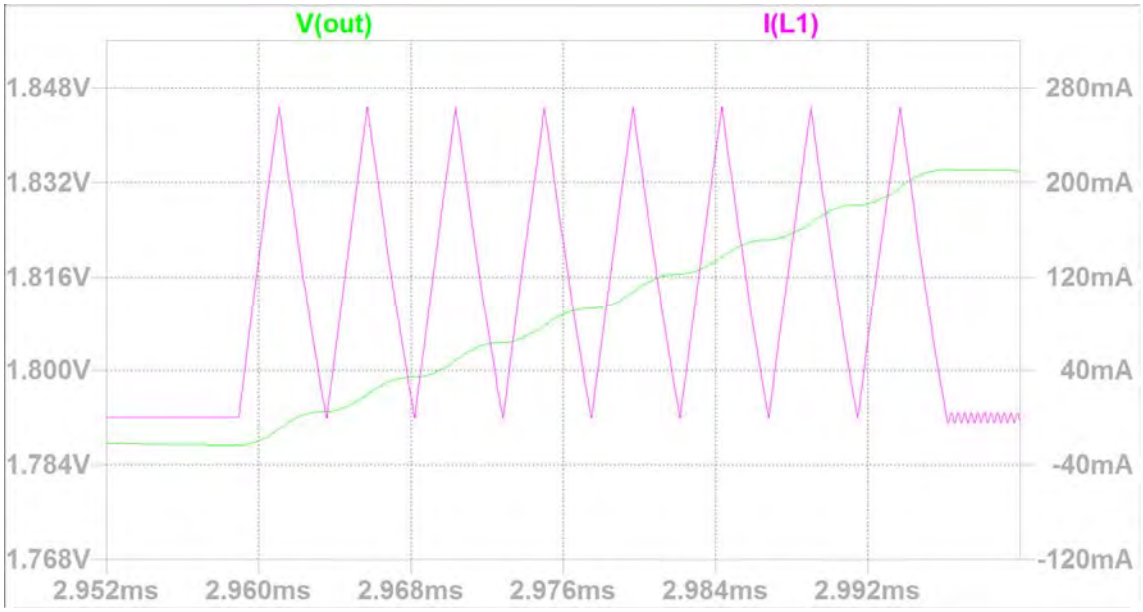

Figure 16. Simulated switching current waveform (measured through L_1) and output voltage (measured at the V_{out} PIN) shown in Figure 11.

THIS PAGE INTENTIONALLY LEFT BLANK

IV. LABORATORY MEASUREMENTS OF PIEZOELECTRIC ENERGY HARVESTER

The measurements and hardware used in the lab to observe the performance of the energy harvesting chip are described in this chapter. The initial laboratory procedures were done to verify the board was not defective and can be found in the specification sheet [12]. Test procedures from the quick start guide were first conducted to verify the board was operating to specifications [12], as shown in Figure 17.

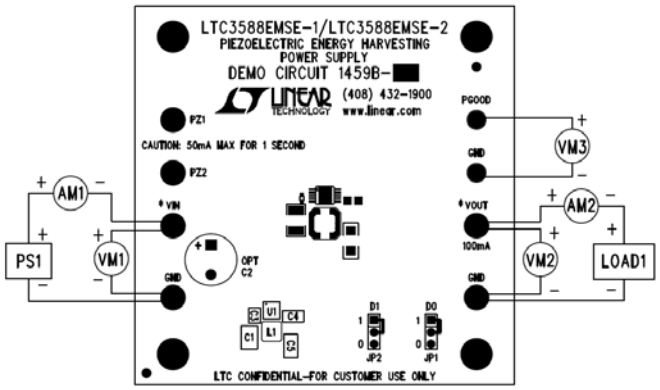

Figure 17. Experimental setup to initially test the demonstration board operation setup (from [12]).

The test equipment used to conduct the measurements is shown in Table 1. The lab bench setup is shown in Figure 18. A picture of the demo board is shown in Figure 19. The demonstration board schematic is shown in Figure 20.

Table 1. Test equipment used for demonstration board observations.

Agilent 33220A 20 MHz function/arbitrary waveform generator
Fluke 45 dual display meter
Tektronix P5200 high voltage differential probe
Tektronix TDS 3014B four channel color digital phosphor oscilloscope
Tektronix TCPA300 amplifier, AC/DC current probe

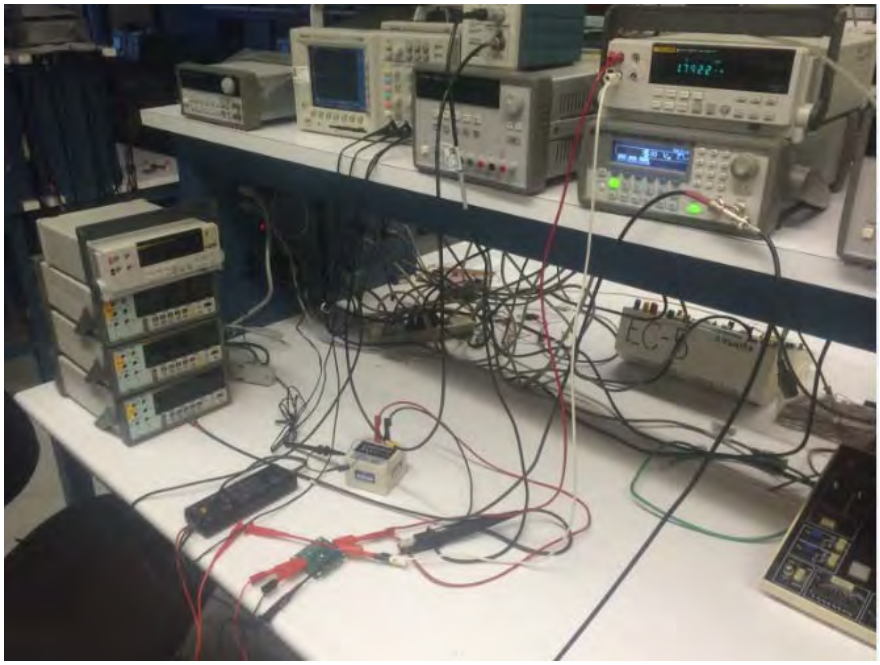

Figure 18. Laboratory bench configuration.

The integrated demonstration board circuit shown in Figure 19 was assembled at Linear Technology. The integrated circuit mounted on the board is the size of a fingernail. This sleek, slim design makes it easy to transport and install.

Figure 19. Demonstration board configuration.

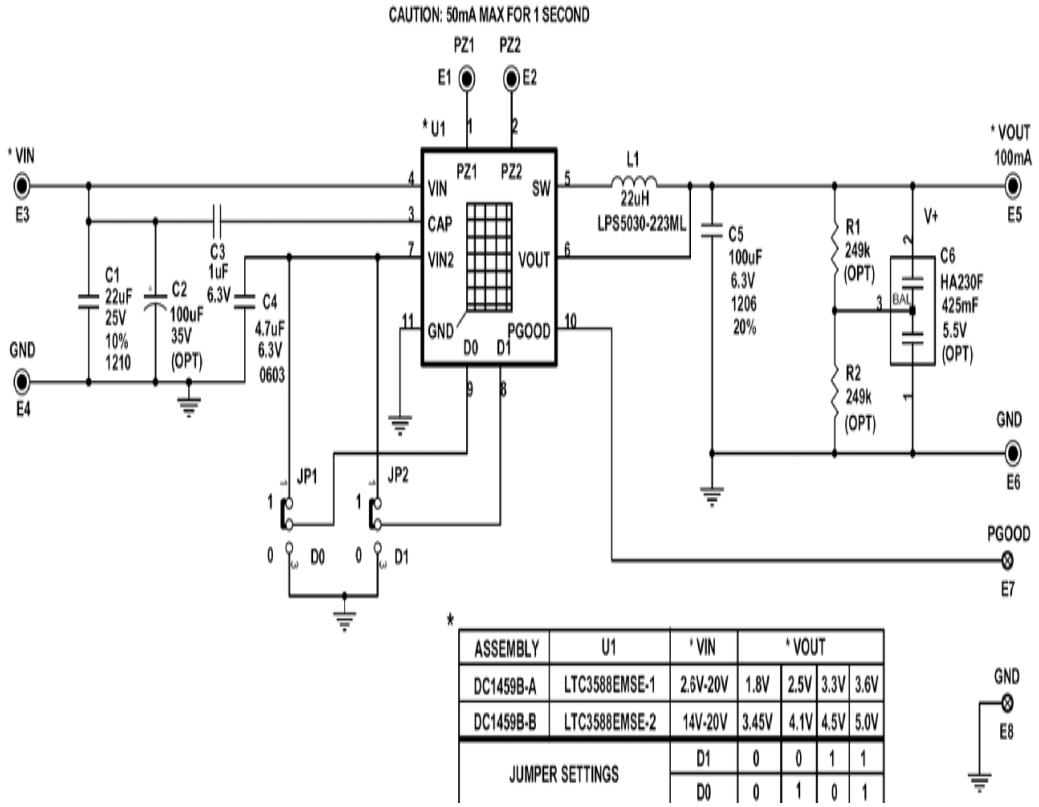

Figure 20. Circuit schematic (from [12]).

Optional capacitors C_2, C_3 and resistors R_1, R_2 shown in Figure 20, were not utilized in this study.

A. RECTIFICATION OF THE AC PIEZO INPUT TO THE ENERGY HARVESTING CHIP

The first stage of the device rectifies the input signal from an AC sine wave into a DC waveform input to the buck chopper. A 30 Hz, $6.0 V_{peak}$ AC voltage representing the piezoelectric input is shown in Figure 21. This input voltage was chosen because it is the worst case scenario for voltage as well as frequency based on research of available piezoelectric material sources [11]. The test case scenario is the worst possible option, meaning any higher frequency or voltage produces better results. The input waveform from the floating function generator connects to the PZ1 and PZ2 connections of the schematic shown in Figure 20. The resulting input voltage waveform is shown in Figure 21.

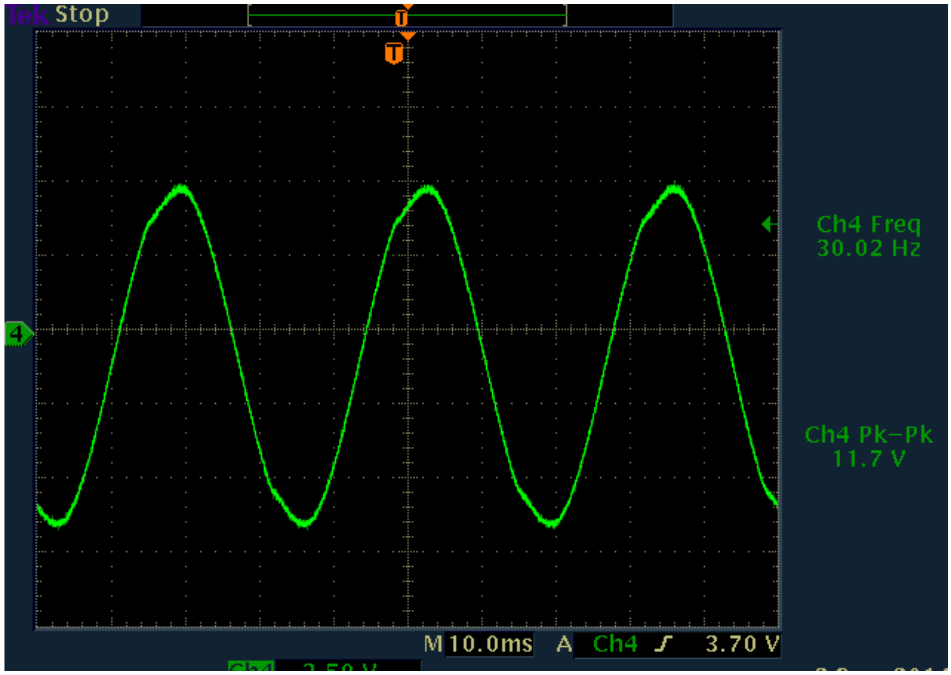

Figure 21. Input to pins PZ1 and PZ2 30 Hz 12V_{pp} sine wave shown in Figure 20.

To understand the next steps in the circuit, we must examine the LTC-3588-1 chip, shown in Figure 22.

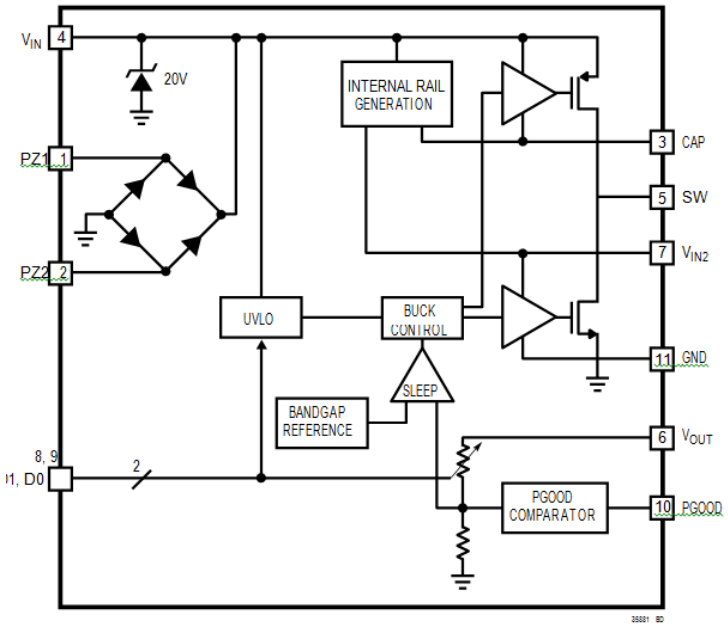

Figure 22. LTC3588-1 integrated circuit block diagram view (from [11]).

The input pins PZ1 and PZ2 are shown connected to a full-wave bridge rectifier represented by four diodes. An oscilloscope measurement was taken from pin 4 of Figure 22, which correlates to pin 4 of Figure 20. The result is shown in Figure 23, where channel 4 is the output voltage of the rectifier with a measured ripple of 1.38 V.

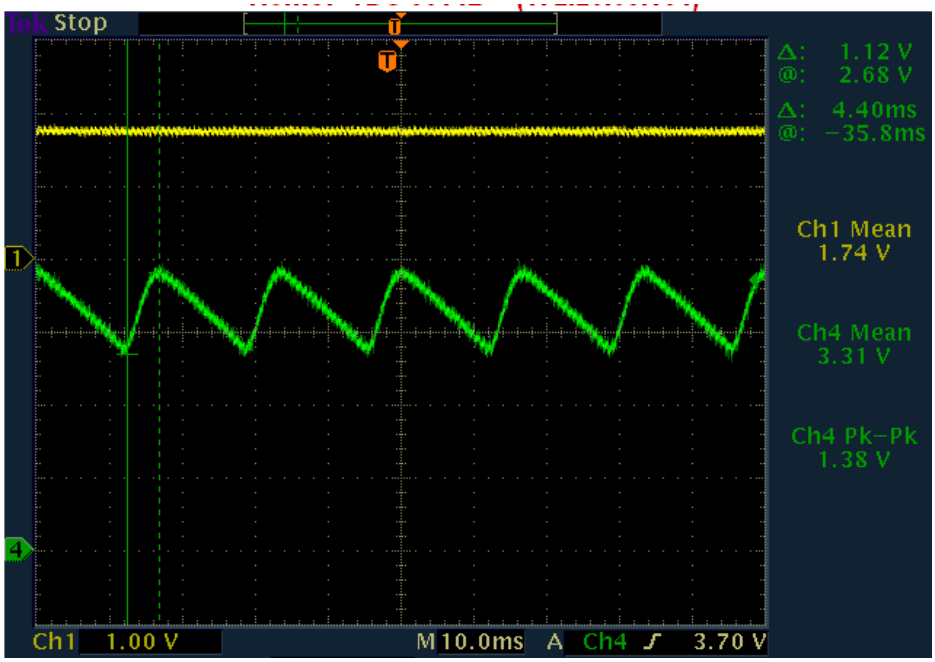

Figure 23. Measured rectified voltage (Ch4) from pin 4 shown in Figure 20 and voltage (Ch1) from the load resistor.

The average value of the rectified output is 3.31 V. The $V_{pk-pk-ripple}$ is the maximum voltage of the ripple, and $V_{rectified\,\mathrm{mean}}$ is the average voltage of the ripple. Calculating $V_{rectified\,\max}$, we get

$$\frac{V_{pk-pk-ripple}}{2} + V_{rectified\,\mathrm{mean}} = V_{rectified\,\max} \tag{14}$$

which equals 4.0 V. We also know the piezoelectric peak input voltage is

$$V_{pzinput} = V_{rectified\,\max} + 2V_{diode}. \tag{15}$$

Rearranging (13), we get

$$V_{pzinput} - V_{rectified\,\max} = 2V_{diode}, \tag{16}$$

and we calculate a V_{diode} drop of 0.55 V for the 500 Ω load case. This voltage drop is consistent with the datasheet voltage drop, as shown in Figure 24 [11]. The bridge current is estimated to be

$$I_{bridge} = \frac{dv}{dt} C_1. \tag{17}$$

The resulting estimated current, 5.6 mA, and the temperature, 25 C, is used with Figure 24 to find the diode bridge voltage drop of 1.1 V from the datasheet [11]. The bridge current path has two diodes in both the positive half-cycle and the negative half-cycle, resulting in two diode voltage drops. Dividing 1.1 V by 2.0, we calculate a 0.55 V drop per diode; this matches within a margin of error to the (16) result. Having two diodes means we expect the voltage drop to be 1.1 V total. Also shown on the input path in Figure 22 is a 20.0 V internal zener diode. This protects the circuit from going above 20.0 V.

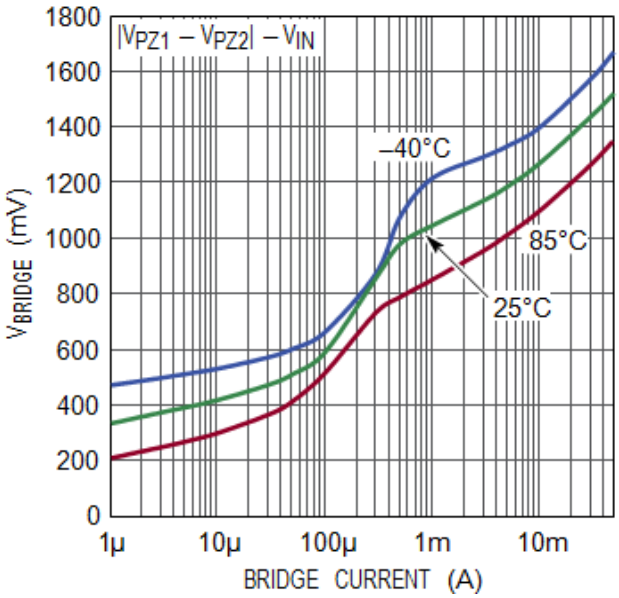

Figure 24. Total bridge rectifier drop vs bridge current (from 9).

The buck chopper component of the circuit is observed from pin 6 of Figure 20 and Figure 22 and is displayed in Figure 23 on channel 1. A *p*-type metal-oxide-semiconductor field-effect transistor PMOS switch from pin 3 and an *n*-type metal-oxide-

semiconductor field-effect transistor NMOS switch from pin 7 is shown in Figure 22. An external capacitor at pin 4 that serves as an input voltage supply for the buck regulator is shown in Figure 20. This capacitor doubles as an energy reservoir that delivers energy during switching. The signal PGOOD on pin 10 was not utilized in this study.

The measured DC value of the output voltage is 1.74 V and is shown in Figure 23. With D0 and D1 set to ground, this is the 1.8 V operation of the device.

B. BUCK CHOPPER

The Buck chopper output voltage of 1.74 V across the load resistor, shown in Figure 25, is the same 1.74 V DC buck chopper voltage shown in Figure 23 except the time axis is set to 100 µs per division. The DC signal is now more easily identified to show a 60 mV ripple with a 1.41 kHz switching frequency F_s. Period is equal to 700 µs as shown in Figure 25.

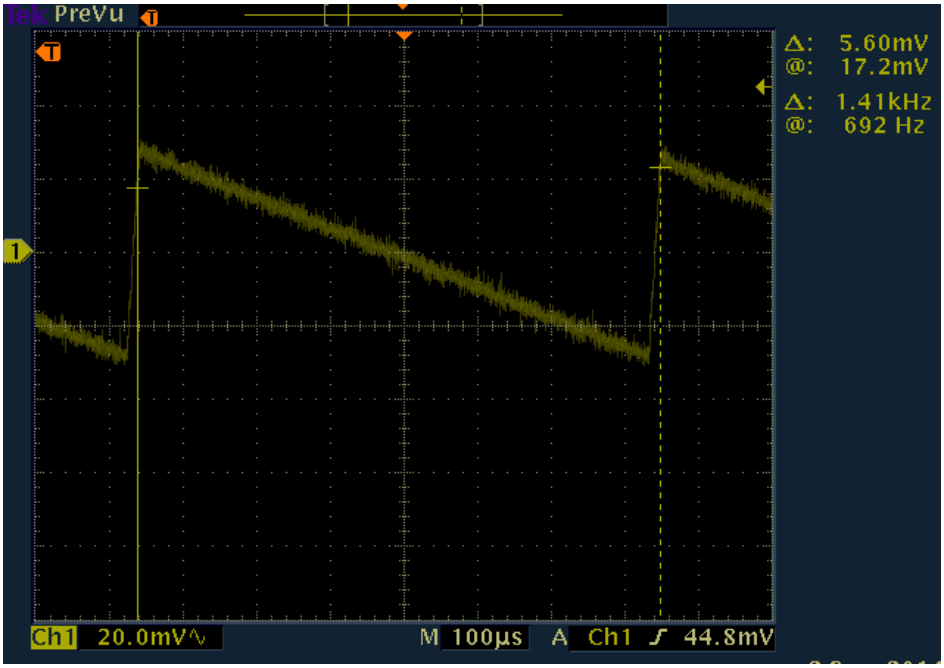

Figure 25. Buck chopper with 500 Ω load. Ch1 measured from load shows 700 µs between pulses.

Under different load conditions, the buck converter changes the switching frequency but maintains the waveform shape, as shown in Figure 26. The fundamental concept remains that the device pulses power to the load to maintain voltage regulation. The period at which this occurs changes depending on the load. We observed that loading down the circuit by a factor of two causes the frequency to increase by roughly a factor of two.

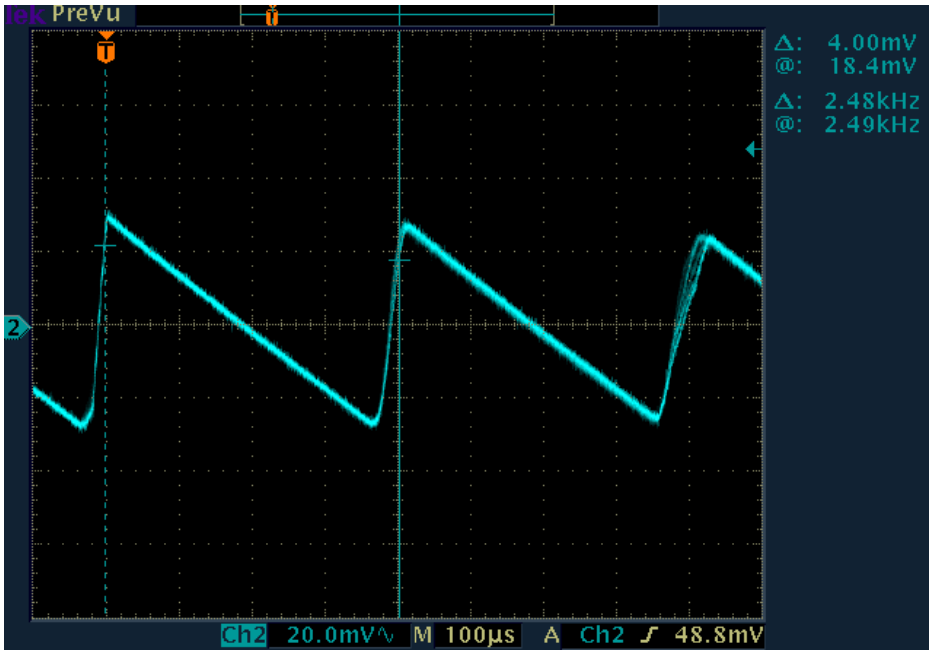

Figure 26. Buck chopper with 250 Ω load. Ch2 measured from load shows 403 µs between pulses.

The effect of shedding the load, or increasing load resistance, is shown in Figures 27, 28, and 29. This linear behavior follows the output load draw of the device. Increasing the load, or lowering the resistance, causes the device to compensate by increasing the frequency at which it turns regulation on and off.

Figure 27. Buck chopper with 1 kΩ load. Ch2 measured from load shows 1.45 ms between pulses.

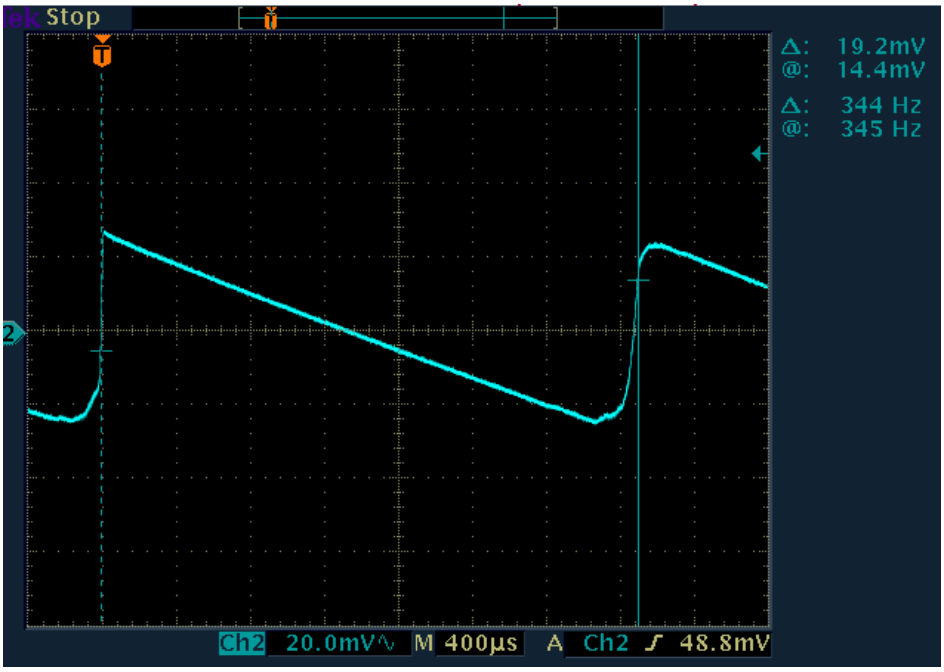

Figure 28. Buck chopper with 2 kΩ load. Ch2 measured from load shows 2.9 ms between pulses.

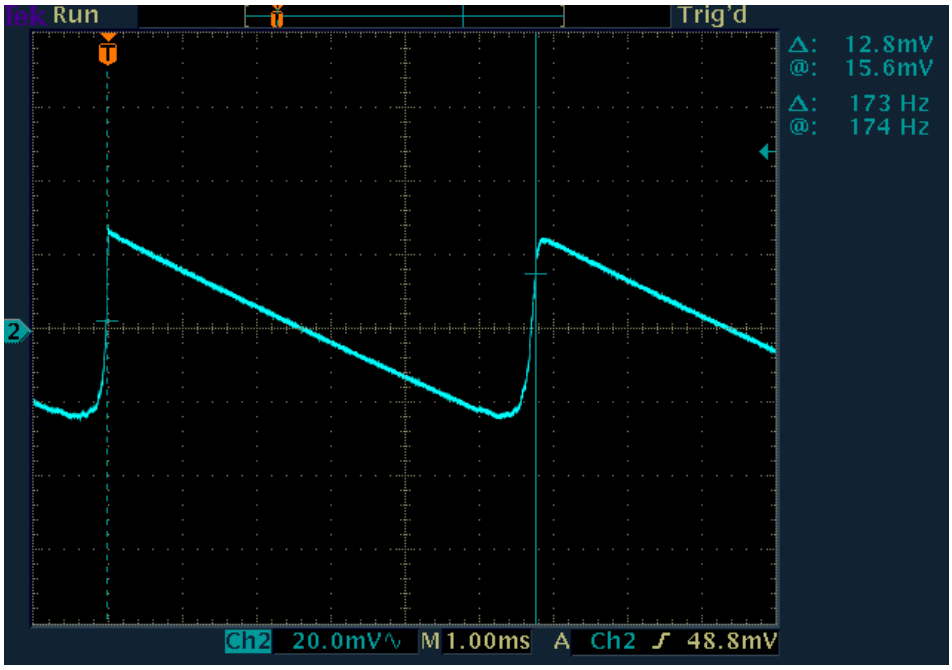

Figure 29. Buck chopper with 4 kΩ load. Ch2 measured from load shows 5.78 ms between pulses.

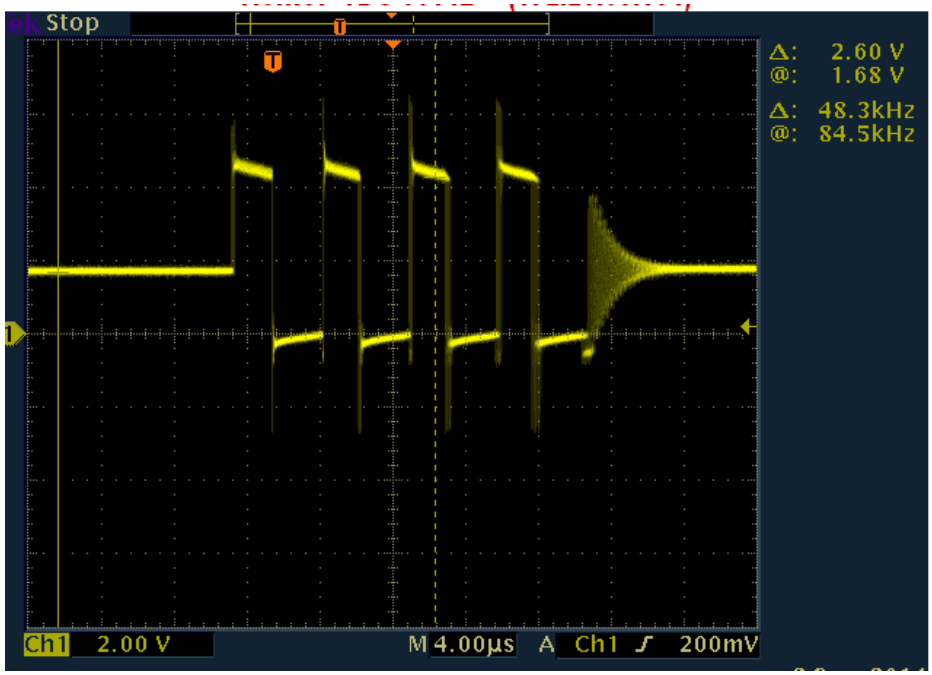

Figure 30. Buck chopper waveform measured from pin 5 shown in Figure 20.

The voltage applied to the inductor by the integrated circuit is shown in Figure 30 with 4 µs per division. This signal is captured using the oscilloscope probe at pin 5 of the

circuit represented by Figure 20, which is the output side of the integrated circuit before the inductor. The buck chopper utilizes pulsed power switching to maintain the output voltage. When the input voltage falls below the under voltage lockout UVLO threshold, the buck converter shuts off. During this time, the output capacitor provides the load energy until it discharges.

There is a sleep comparator shown in Figure 22 that monitors the output voltage. When the output voltage falls below the regulation point, the buck regulator wakes up and provides a burst of energy. This cycle repeats itself and is used to regulate the output voltage.

The LTC-3588-1 device keeps the NMOS switch on during the comparator sleep threshold period; this prevents the conduction loss that normally occurs in the body diode. If the PMOS is on when the sleep comparator turns on, the NMOS turns on to drive the current down to zero. The NMOS is what makes the device energy efficient. The pulsing behavior of the LTC3588-1 is observed by changing the load values while observing pin 5 of Figure 20, as shown in Figures 31, 32, 33, and 34.

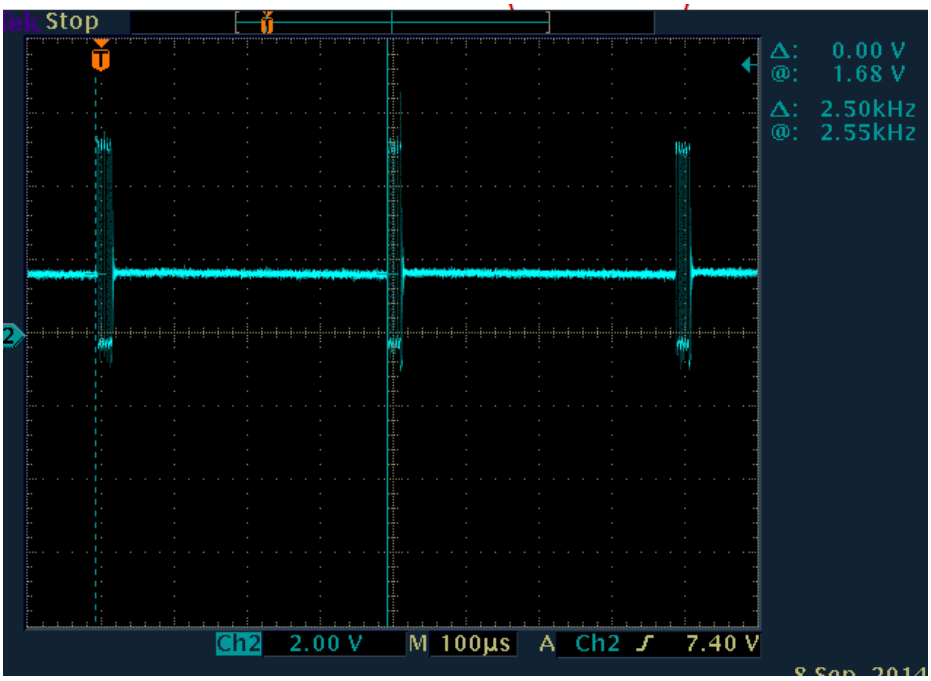

Figure 31. Chip voltage at pin 5 shown in Figure 20 with 250 Ω load. Ch2 shows 4.0 µs between pulses.

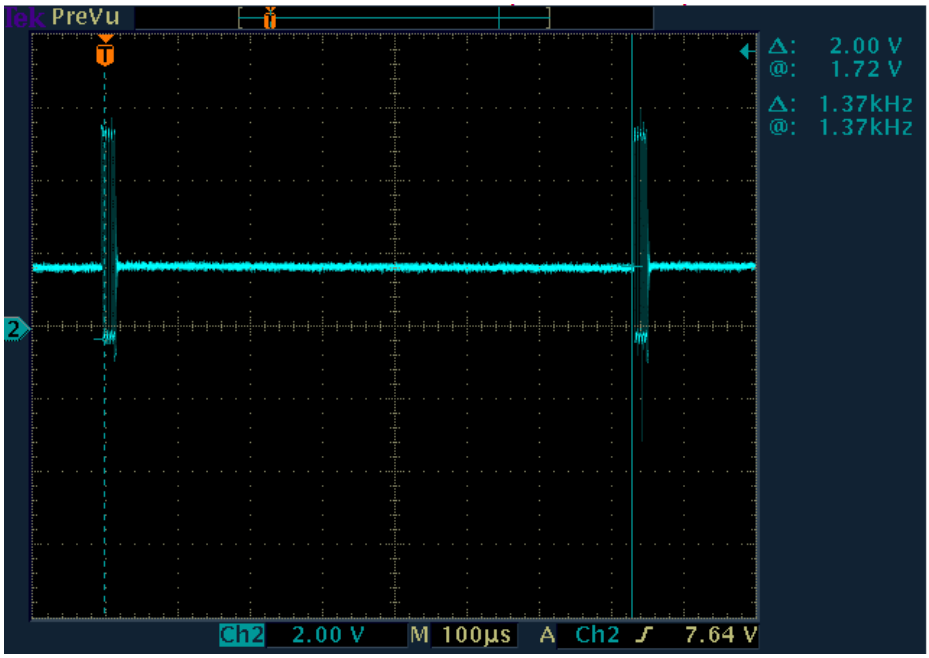

Figure 32. Chip voltage at pin 5 shown in Figure 20 with 500 Ω load. Ch2 shows 7.3 µs between pulses.

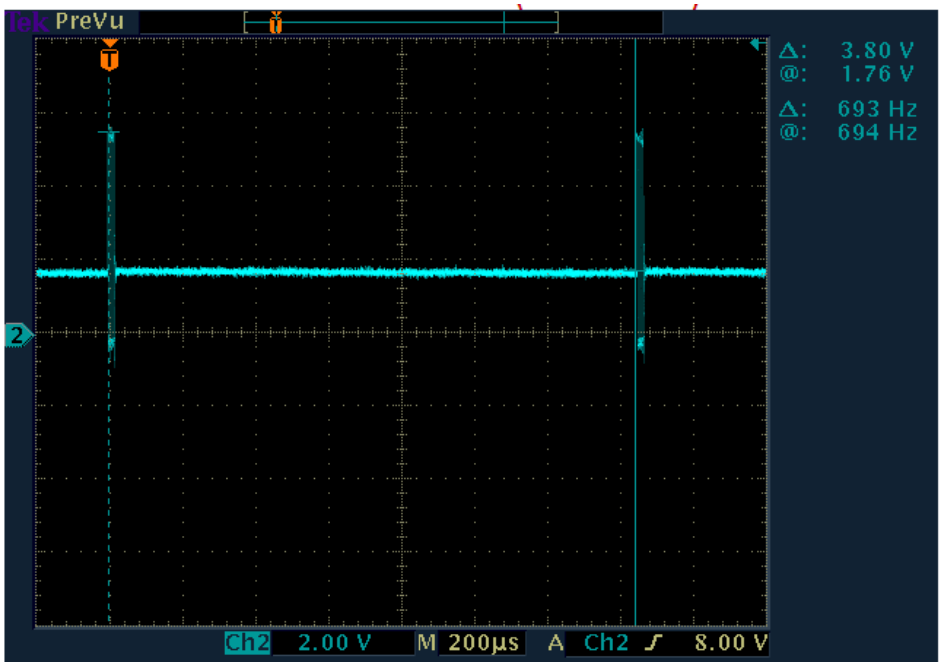

Figure 33. Chip voltage at pin 5 shown in Figure 20 with 1 kΩ load. Ch2 shows 1.43 ms between pulses.

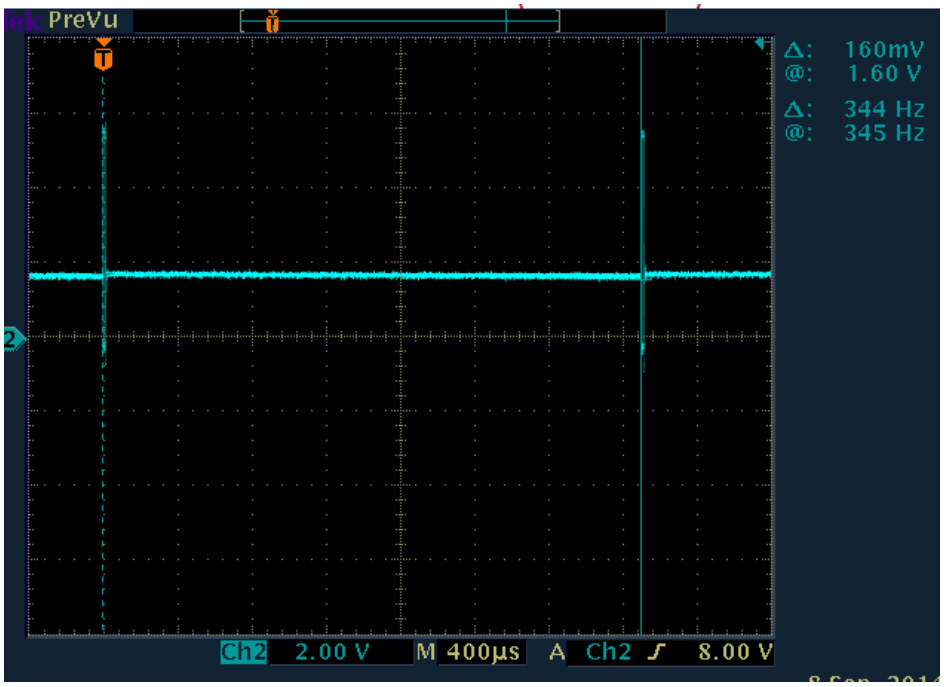

Figure 34. Chip voltage at pin 5 shown in Figure 20 with 2 kΩ load. Ch2 shows 2.91 ms between pulses.

The energy transfer to the load only occurs at times where there is sufficient energy at the input capacitor, and, thus, the time it takes to transfer the power to the load is much shorter than the time it takes the device to harvest the energy. This makes the device ideal for harvesting small amounts of energy for a longer period of time.

The four selectable voltage outputs are controlled by the jumpers JP1 and JP2 in Figure 20. The four voltage options are 1.8 V, 2.5 V, 3.3 V, and 3.6 V.

The resulting measurement of the circuit operation is shown in Figure 35. Unlike the simulation, we were unable to measure the inductor current because the inductor is a surface mounted part on the board. The simulation results shown in Figure 16 give a clearer picture of the voltage steps and the inductor current behavior. The added noise in the measurement shown in Figure 35 is due to equipment error, noise and calibration. The 60.2 mV ripple shown in Figure 35 depicts the regulation of the buck chopper. Once the voltage reaches the regulation minimum, the chopper sends a pulse of power, reassesses, and sends another pulse of power if necessary to reach the cutoff voltage. Once the

voltage is regulated to the desired value, the buck chopper turns off and monitors the output voltage until it again reaches the minimum threshold. This process repeats.

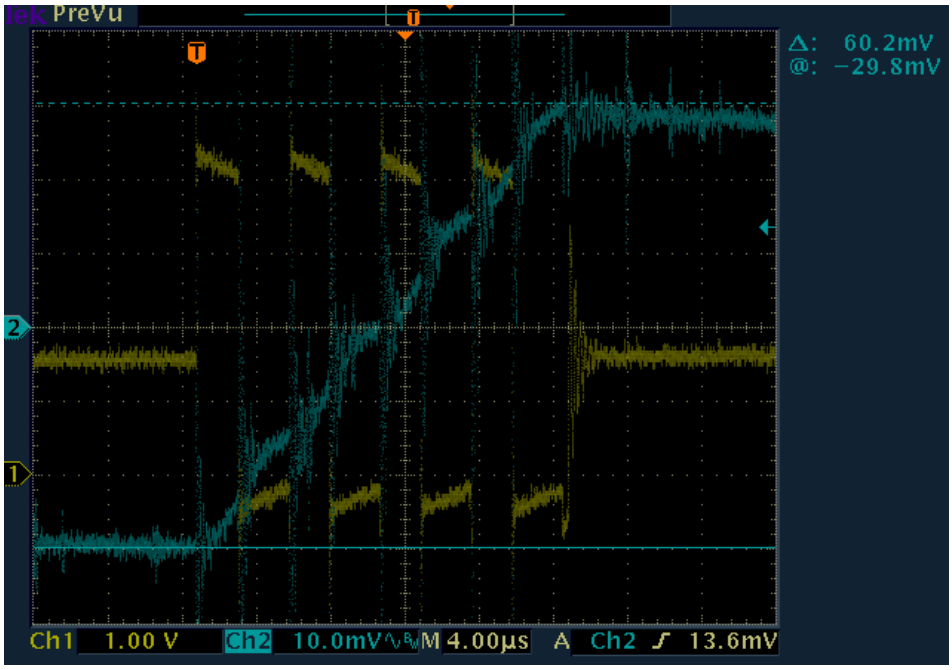

Figure 35. Measured output voltage from switching and the pin 5 voltage shown in Figure 20 (Ch1) and load resistor voltage (Ch2).

C. POWER OUTPUT

The function generator serves as the voltage source for the energy harvester. The function generator voltage and current were measured, and the waveforms are shown in Figure 36. When the voltage and current are multiplied together, the average value is the estimate of the input electrical power. Measuring the voltage and current from the load resistor, we calculated the output power as shown in Figure 37. The output power was measured to be 5.3 mW, enough to power a GPS transceiver or other small power device.

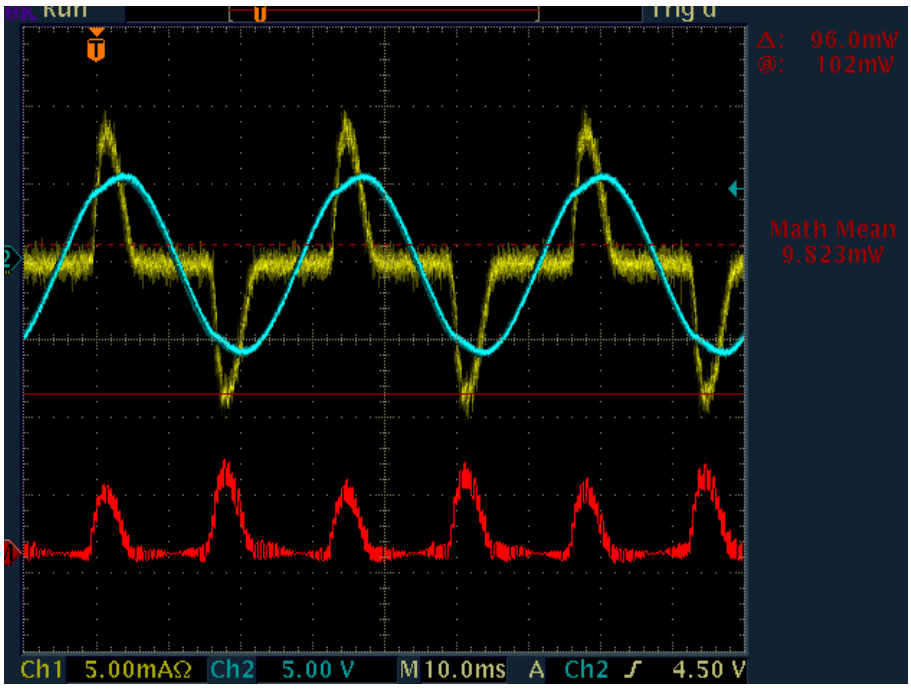

Figure 36. Input current (Ch1), voltage (Ch2) and output power (ChM) measured from the function generator.

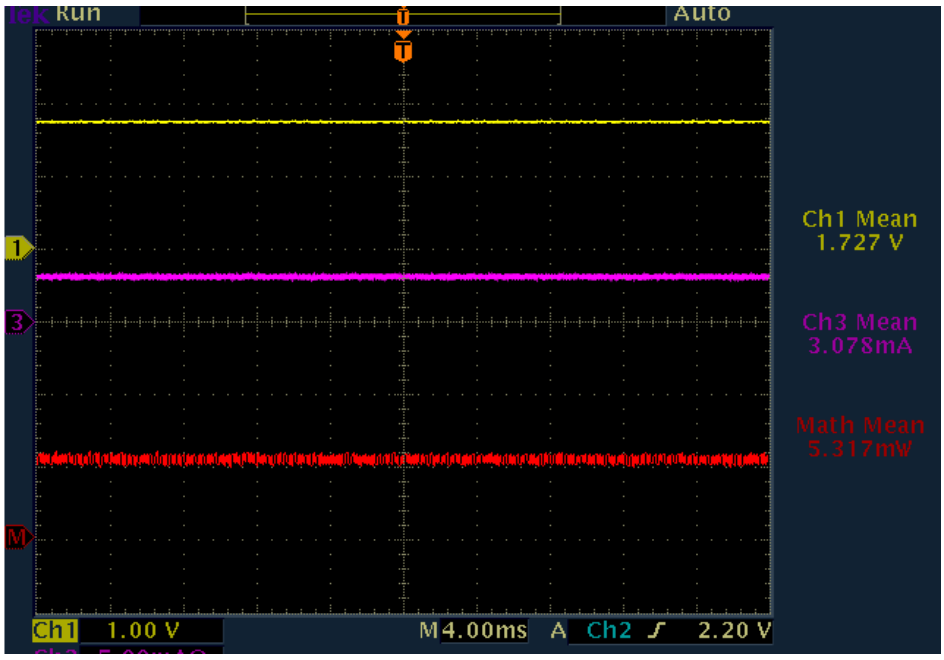

Figure 37. The voltage (Ch1) and current (Ch3) of the load resistor and the output power (ChM).

The efficiency is estimated to be 54%. This may be inaccurate due to instrumentation calibration errors. This number is not as important keeping in mind that this is free energy.

D. CORRELATION BETWEEN HARDWARE, TEXTBOOK AND SIMULATION

Putting the laboratory demonstration, textbook example and software simulation together, the LTC3588-1 performs to specification. The full-bridge rectification shown in Figures 38, 39, and 40 correlate between laboratory demonstration, textbook example and software simulation.

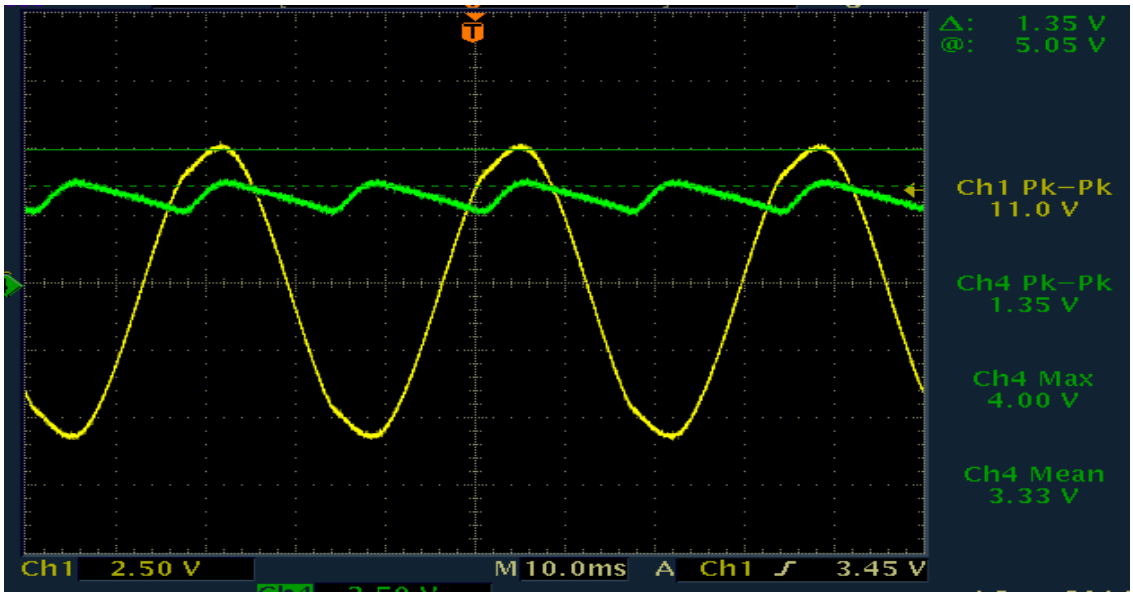

Figure 38. Rectification demonstration.

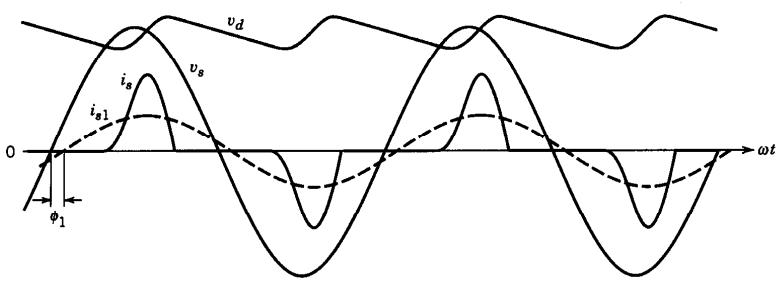

Figure 39. Textbook rectification example (from [9]).

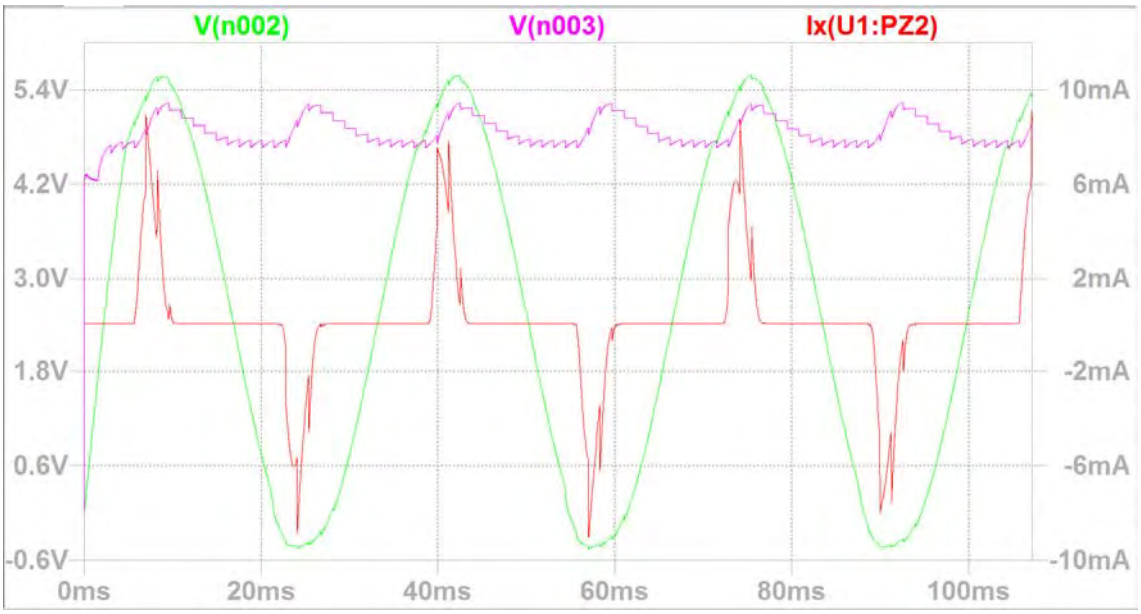

Figure 40. LTSpiceIV simulation with v_s (green), v_d (purple) and i_s (red).

This correlation between textbook, demonstration and software simulation validates the use of software design to test product behavior prior to construction. The LTSpiceIV program is a reliable tool to predict the device performance.

THIS PAGE INTENTIONALLY LEFT BLANK

V. CONCLUSION AND FUTURE WORK

Two blocks of power electronics (full-bridge rectifier and buck chopper) were combined in this thesis to use a simulated piezoelectric voltage source and harvest the energy to a resistor load.

A. CONCLUSION

Simulation and laboratory demonstration both verify the ability of the LTC3588-1 integrated circuit chip to harvest an AC waveform input and transfer power to a resistor load. Laboratory equipment calibration was needed prior to conducting measurements as well as floating the function generator. LTSpiceIV software was easy to download and install. The use of the LTSpiceIV software provided insight into circuit behavior, especially the case where the inductor current cannot be measured. The parameters for the simulated source input can be found from Piezo Inc [13].

B. FUTURE WORK

The output pin PGOOD of the device was not used. According to the specification sheet, we see that this tells the user when the converter is in operation.

This energy harvesting chip produces a small voltage DC power that can be used in many ways. A resistor was used as the load case in my research. Future work could connect a battery to the output to be charged.

While 5.3 mW of power is not much, the LTC-3588-1 is smaller than a finger nail. Further study into combining several inputs and devices can be accomplished to investigate the ability to daisy chain either multiple sources or harvesters.

THIS PAGE INTENTIONALLY LEFT BLANK

LIST OF REFERENCES

[1] R. Mabus. “SECNAV Instruction 4101.3” [Online]. Available: http://www.secnav.navy.mil/eie/ASN%20EIE%20Policy/4101.3.pdf (accessed August 2014).

[2] P. Cullom. “Task force energy charter” [Online]. Available: http://greenfleet.dodlive.mil/files/2010/10/TFE_Charter.pdf (accessed August 2014).

[3] Naval Postgraduate School. “2013 Naval Postgraduate School annual report” [Online]. Available: http://www.nps.edu/About/Publications/Annual%20Report%202013/YearinReview2013.pdf (accessed August 2014).

[4] A. Cabiling, “Ultra low-voltage energy harvesting,” M.S. thesis, Dept Electrical and Computer Eng., Naval Postgraduate School, Monterey, CA 2013.

[5] N. Hoffman, “A miniature electromechancial generator design utilizing human motion,” M.S. thesis, Dept Electrical and Computer Eng., Naval Postgraduate School, Monterey, CA 2010.

[6] S. Forester, “Energy harvesting for self-powered, ultra-low power microsystems with focus on vibration-based electromechanical conversion,” M.S. thesis, Dept Computer Science, Naval Postgraduate School, Monterey, CA 2009.

[7] T. Huq, and S. Williamson, “Comprehensive comparative analysis of piezoelectric energy harvesting circuits for battery charging applications,” IEEE Industrial Electronics Society, IECON 2013.

[8] G. Ottman, H. Hoffman, A. Bhatt, and G. Lesieutre, “Adaptive piezoelectric energy harvesting circuit for wireless remote power supply,” *IEEE Trans. Power Electron.*, vol 17 no.5 September 2002.

[9] N. Mohan, T. Undeland, and W. Robbins. *Power Electronics. Converters, Applications, and Design*. Hoboken, NJ: John Wiley & Sons, Inc. 2003.

[10] M. Fisher, *Power Electronics*. Boston, MA: PWS Kent, 1991.

[11] Linear Technology, “LTC3588-1 datasheet,” in *LTC3588-1 Nano Energy Harvesting Power Supply*. Milpitas, CA: Linear Technology, April 2010.

[12] Linear Technology, Demo Circuit 1459b quick start guide [user’s guide]. Milpitas, CA: Linear Technology, April 2010.

[13] Piezo Systems, “Piezoelectric Energy Harvesting Kit.” Woburn, MA: Piezo Systems, Inc.

THIS PAGE INTENTIONALLY LEFT BLANK

INITIAL DISTRIBUTION LIST

1. Defense Technical Information Center
   Ft. Belvoir, Virginia

2. Dudley Knox Library
   Naval Postgraduate School
   Monterey, California